

# Th1 cells downregulate connexin 43 gap junctions in astrocytes via microglial activation

渡邊, 充

<https://doi.org/10.15017/1806891>

---

出版情報：九州大学, 2016, 博士 (医学), 課程博士  
バージョン：  
権利関係：全文ファイル公表済

# SCIENTIFIC REPORTS



OPEN

## Th1 cells downregulate connexin 43 gap junctions in astrocytes via microglial activation

Mitsuru Watanabe<sup>1</sup>, Katsuhisa Masaki<sup>1</sup>, Ryo Yamasaki<sup>1</sup>, Jun Kawanokuchi<sup>2,3</sup>, Hideyuki Takeuchi<sup>2,4</sup>, Takuya Matsushita<sup>1</sup>, Akio Suzumura<sup>2</sup> & Jun-ichi Kira<sup>1</sup>

Received: 14 July 2016  
Accepted: 08 November 2016  
Published: 08 December 2016

We previously reported early and extensive loss of astrocytic connexin 43 (Cx43) in acute demyelinating lesions of multiple sclerosis (MS) patients. Because it is widely accepted that autoimmune T cells initiate MS lesions, we hypothesized that infiltrating T cells affect Cx43 expression in astrocytes, which contributes to MS lesion formation. Primary mixed glial cell cultures were prepared from newborn mouse brains, and microglia were isolated by anti-CD11b antibody-conjugated magnetic beads. Next, we prepared astrocyte-rich cultures and astrocyte/microglia-mixed cultures. Treatment of primary mixed glial cell cultures with interferon (IFN)  $\gamma$ , interleukin (IL)-4, or IL-17 showed that only IFN  $\gamma$  or IL-17 at high concentrations reduced Cx43 protein levels. Upon treatment of astrocyte-rich cultures and astrocyte/microglia-mixed cultures with IFN  $\gamma$ , Cx43 mRNA/protein levels and the function of gap junctions were reduced only in astrocyte/microglia-mixed cultures. IFN  $\gamma$ -treated microglia-conditioned media and IL-1 $\beta$ , which was markedly increased in IFN  $\gamma$ -treated microglia-conditioned media, reduced Cx43 protein levels in astrocyte-rich cultures. Finally, we confirmed that Th1 cell-conditioned medium decreased Cx43 protein levels in mixed glial cell cultures. These findings suggest that Th1 cell-derived IFN  $\gamma$  activates microglia to release IL-1 $\beta$  that reduces Cx43 gap junctions in astrocytes. Thus, Th1-dominant inflammatory states disrupt astrocytic intercellular communication and may exacerbate MS.

Connexins (Cxs) are a family of vertebrate proteins that form gap junction (GJ) channels, the major intercellular channel that facilitates direct signalling between cytoplasmic compartments of adjacent cells. A GJ consists of a pair of hemichannels, each of which is a hexameric cluster of Cxs. Various tissues and cell types exhibit characteristic Cx expression profiles. In the central nervous system (CNS), there are abundant GJs between adjacent astrocytes (A/A junctions) and between oligodendrocytes and astrocytes (O/A junctions)<sup>1–3</sup>. Astrocytes are functionally coupled to adjacent astrocytes and oligodendrocytes by GJs and form the “glial syncytium” that maintains the homeostasis of glial and neuronal cells<sup>4</sup>. Cx43 is regarded as the primary astrocytic GJ protein<sup>5,6</sup>. Cx43 is diffusely expressed in the fine processes of cortical astrocytes in grey matter<sup>7</sup>. In white matter, Cx43 expression levels are lower than in grey matter, and Cx43 is present in the foot processes of perivascular astrocytes<sup>7–9</sup>.

Multiple sclerosis (MS) is an inflammatory demyelinating disease of the CNS. The pathological hallmark of MS is demyelinating plaques with relatively preserved axons, suggesting that autoimmune responses preferentially target CNS myelin. We previously reported early and extensive loss of astrocytic Cx43 in active white matter lesions of MS, neuromyelitis optica (NMO), and Baló’s concentric sclerosis (BCS) patients<sup>10–12</sup>. It has been suggested that early disruption of cell-to-cell communications among glial cells may have a crucial role in the development of demyelinating plaques<sup>12–14</sup>. Perivascular lymphocytic cuffing mainly consisting of T cells has been observed significantly more frequently in active demyelinating lesions with Cx43 loss<sup>11</sup>. Moreover, Cx43 loss is significantly associated with a rapidly progressive disease course, culminating in death<sup>11</sup>. Although some proinflammatory factors have been reported to reduce astrocytic expression of Cx43 *in vitro*<sup>15</sup>, the mechanisms of Cx43 loss remain to be elucidated in demyelinating diseases. Because it is widely accepted that autoimmune T cells are involved in the pathogenesis of MS and experimental autoimmune encephalomyelitis (EAE), an animal

<sup>1</sup>Department of Neurology, Neurological Institute, Graduate School of Medical Sciences, Kyushu University, Fukuoka, 812-8582, Japan. <sup>2</sup>Department of Neuroimmunology, Research Institute of Environmental Medicine, Nagoya University, Nagoya, 464-8601, Japan. <sup>3</sup>Institute of Traditional Chinese Medicine, Suzuka University of Medical Science, Suzuka, 510-0226, Japan. <sup>4</sup>Department of Neurology and Stroke Medicine, Yokohama City University Graduate School of Medicine, Yokohama, 236-0004, Japan. Correspondence and requests for materials should be addressed to J.-I.K. (email: kira@neuro.med.kyushu-u.ac.jp)

model of MS<sup>16</sup>, we hypothesized that infiltrating T cells might alter Cx43 protein levels in astrocytes and contribute to MS lesion extension. In this study, we investigated whether CD4<sup>+</sup> T cells, such as T helper (Th) 1, Th17, or regulatory T (Treg) cells, directly or indirectly influence Cx43 protein levels in astrocytes using a primary glial cell culture system.

## Results

**Cell types in mixed or purified glial cell cultures.** Primary mixed glial cell cultures were prepared from the brains of newborn C57BL/6 J mice. Primary mixed glial cell cultures contained  $36.6 \pm 11.1\%$  ionized calcium-binding adapter molecule-1 (Iba-1)-positive microglia (five independent experiments), and the remaining cells were almost all glial fibrillary acidic protein (GFAP)-positive astrocytes (Supplementary Fig. S1a). We detected Cx43 on the surface of astrocytes by immunocytochemistry (Supplementary Fig. S1b). Cx30 was not detected in these cultures (Supplementary Fig. S1c). Microglia were isolated from these primary mixed glial cell cultures by anti-CD11b antibody (Ab)-conjugated magnetic beads. Microglial cultures contained  $>90\%$  Iba-1-positive cells ( $94.6 \pm 2.8\%$ , five independent experiments) (Supplementary Fig. S1d). Next, we prepared astrocyte-rich cultures and astrocyte/microglia-mixed cultures (Supplementary Fig. S1e–f). Astrocyte-rich cultures contained  $<2\%$  Iba-1-positive cells ( $0.7 \pm 0.7\%$ , nine independent experiments). Astrocyte/microglia-mixed cultures contained  $38.2 \pm 2.1\%$  (five independent experiments) Iba-1-positive cells when they were used for the following experiments. All of these cultures contained no NeuN-positive cells (neurons),  $<1\%$  Nogo-A-positive cells (oligodendrocytes), and  $<1\%$  neuron-glial antigen 2 (NG2)-positive cells (oligodendrocyte precursors) (Supplementary Fig. S1g–i).

**Interferon (IFN) $\gamma$  downregulates Cx43 protein levels in mixed glial cell cultures.** Primary mixed glial cell cultures were treated with recombinant mouse IFN $\gamma$ , interleukin (IL)-4, and IL-17, which are produced mainly by Th1, Th2, and Th17 cells, respectively, at concentrations of 0 (control), 5, 50, or 500 ng/ml for 24 h. Western blotting revealed that IFN $\gamma$  reduced Cx43 protein levels in a dose-dependent manner, and that IL-17 at the highest concentration only (500 ng/ml) reduced Cx43 protein levels, whereas IL-4 did not affect Cx43 protein levels at any tested concentration (Fig. 1).

**IFN $\gamma$  decreases astrocytic Cx43 protein and mRNA levels only in the presence of microglia.** Because primary mixed glial cell cultures contained mainly astrocytes and microglia, we next examined whether IFN $\gamma$  reduced Cx43 protein and mRNA levels in astrocytes directly or via microglia. Upon treatment of astrocyte-rich cultures with IFN $\gamma$  for 24 h, the protein and mRNA levels of Cx43 were unchanged (Fig. 2a,c,e). In contrast, upon treatment of astrocyte/microglia-mixed cultures with IFN $\gamma$  for 24 h, the reduction of Cx43 protein and mRNA levels was dose dependent (Fig. 2b,d,f). Upon treatment of astrocyte-rich cultures and astrocyte/microglia-mixed cultures with IL-17 for 24 h, only the highest concentration of IL-17 reduced the protein levels of Cx43 in astrocyte/microglia-mixed cultures, but not in astrocyte-rich cultures (Fig. 3). These observations implied that both IFN $\gamma$  and IL-17 reduced Cx43 protein and mRNA levels in astrocytes via microglia. Because IL-17 only affected Cx43 protein levels at extremely high concentrations, we focused on the effects of IFN $\gamma$  on glial cells in the following experiments.

**Microglia activated by IFN $\gamma$  suppress the function of GJs in astrocytes.** We next assessed the functional states of GJs using a scrape loading/dye transfer (SLDT) assay. Upon treatment of astrocyte-rich cultures and astrocyte/microglia-mixed cultures with IFN $\gamma$  for 24 h, the functions of GJs were significantly suppressed in astrocyte/microglia-mixed cultures, but not in astrocyte-rich cultures (Fig. 4).

**Humoural factors secreted from IFN $\gamma$ -activated microglia decrease Cx43 protein levels in astrocytes.** Next, microglial cultures were treated with IFN $\gamma$  and their supernatants were collected after 24 h (IFN $\gamma$ -treated microglia-conditioned media). Resting microglia had a rod shape, whereas IFN $\gamma$ -treated microglia showed morphological changes including a large and round, amoeboid shape (Supplementary Fig. S2). When IFN $\gamma$ -treated microglia-conditioned media were applied to astrocyte-rich cultures, astrocytic Cx43 protein levels were significantly downregulated after 24 h (Fig. 5). These findings suggest that IFN $\gamma$  activates microglia, and that humoural factors secreted from activated microglia decrease Cx43 protein levels in astrocytes.

**Identification of humoural factors that decrease Cx43 protein levels in astrocytes.** To identify the humoural factors secreted from activated microglia, we focused on several cytokines and chemokines, and measured their concentrations in IFN $\gamma$ -treated microglia-conditioned media using a Bio-Plex Multiplex System. IFN $\gamma$  treatment significantly enhanced microglial secretion of all measured cytokines and chemokines in a dose-dependent manner (Fig. 6 and Supplementary Fig. S3). In particular, we focused on IL-1 $\beta$ , IL-6, and tumour necrosis factor (TNF) $\alpha$  that were present in IFN $\gamma$ -treated microglia-conditioned media at high concentrations (peak values:  $>100$  pg/ml) and have been reported as representative proinflammatory cytokines secreted from activated microglia<sup>17–19</sup>. We treated astrocyte-rich cultures with either IL-1 $\beta$ , IL-6, or TNF $\alpha$  for 24 h. IL-1 $\beta$  significantly reduced Cx43 protein levels in astrocytes in a dose-dependent manner (Fig. 7a, Supplementary Fig. S4). However, upon treatment of astrocyte-rich cultures with combinations of these cytokines, not only IL-1 $\beta$  and IL-6 or TNF $\alpha$ , but also IL-6 and TNF $\alpha$  reduced astrocytic Cx43 protein levels, although IL-6 or TNF $\alpha$  alone did not change Cx43 protein levels (Fig. 7b). Therefore, the main humoural factor secreted from microglia, which decreases Cx43 protein levels in astrocytes, is IL-1 $\beta$ , whereas only IL-6 and TNF $\alpha$  in combination decreases astrocytic Cx43 protein levels.

**Culture supernatants of Th1 cells downregulate Cx43 protein levels in mixed glial cell cultures.** Next, we examined whether Th1 cells reduced Cx43 protein levels in mixed glial cell cultures. Stocks of

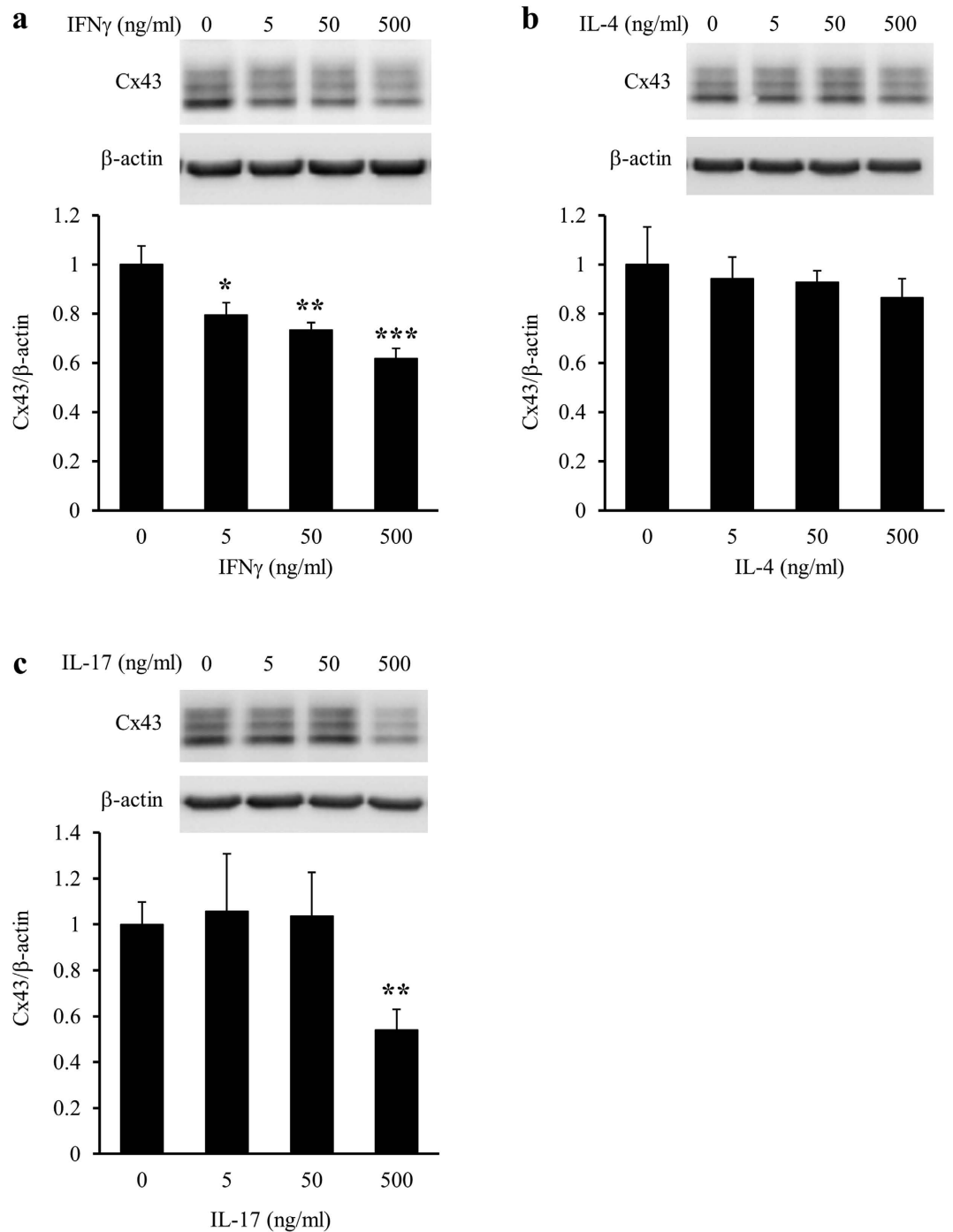


**Figure 1. Effects of IFN $\gamma$ , IL-4, and IL-17 treatments on Cx43 protein levels in primary mixed glial cell cultures.** Primary mixed glial cell cultures were treated with the vehicle (0) or 5, 50, and 500 ng/ml IFN $\gamma$  (a), IL-4 (b), or IL-17 (c) for 24 h. Cx43 protein levels in primary mixed glial cell cultures were assessed by western blotting.  $\beta$ -actin was used as a loading control. Cx43/ $\beta$ -actin of the vehicle treatment was set as 1. Data are presented as the mean  $\pm$  s.d. (n = 4, \* $p$  < 0.05, \*\* $p$  < 0.01, and \*\*\* $p$  < 0.001, compared with the vehicle-treated control by one-way ANOVA followed by Dunnett's multiple comparison test). Full-length blots are presented in Supplementary Fig. S6.

conditioned media from Th1, Th17, and Treg cells differentiated from naive T cells *in vitro* contained 444.6, 0.1, and 3.2 ng/ml IFN $\gamma$ , respectively, as measured by enzyme-linked immunosorbent assay (ELISA). IFN $\gamma$  was not detected in glial medium (GM) or complete RPMI medium. Primary mixed glial cell cultures were treated with conditioned media from individual T cell subsets for 24 h, and then changes in Cx43 protein levels were quantified by western blotting. As shown in Fig. 8, only Th1 cell-conditioned medium significantly reduced Cx43

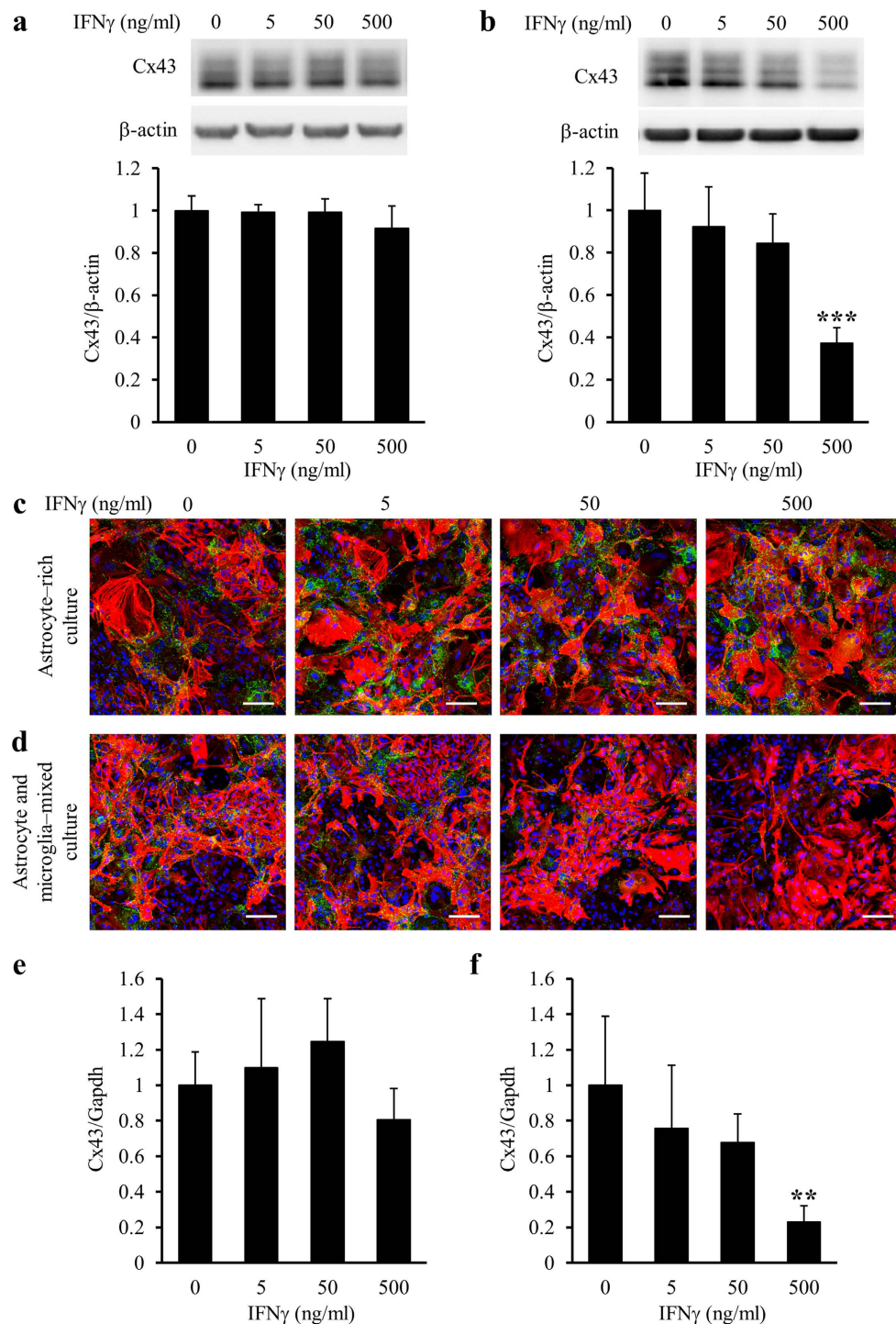


**Figure 2. Difference in the effects of IFN $\gamma$  on Cx43 protein and mRNA levels in the presence or absence of microglia in cultures.** Astrocyte-rich cultures (a,c,e) and astrocyte/microglia-mixed cultures (b,d,f) were treated with the vehicle (0) or 5, 50, and 500 ng/ml IFN $\gamma$  for 24 h. (a,b) Cx43 protein levels were assessed by western blotting.  $\beta$ -actin was used as a loading control. Cx43/ $\beta$ -actin of the vehicle treatment was set as 1. Data are presented as the mean  $\pm$  s.d. (n = 4, \*\*\* $p$  < 0.001, compared with the vehicle-treated control by one-way ANOVA followed by Dunnett's multiple comparison test). Full-length blots are presented in Supplementary Fig. S7. (c,d) Cx43 protein levels were assessed by immunocytochemical staining. Fixed cells were immunostained for Cx43 (green) and GFAP (red), and counterstained with DAPI (blue). Scale bars: 100  $\mu$ m. (e,f) Cx43 (*Gja1*) mRNA levels were analysed by quantitative real-time RT-PCR. The expression of Cx43 mRNA was normalized to that of Gapdh mRNA as an internal control. Cx43/Gapdh of the vehicle treatment was set as 1. Data are presented as the mean  $\pm$  s.d. (n = 4, \*\* $p$  < 0.01, compared with the vehicle-treated control by one-way ANOVA followed by Dunnett's multiple comparison test).



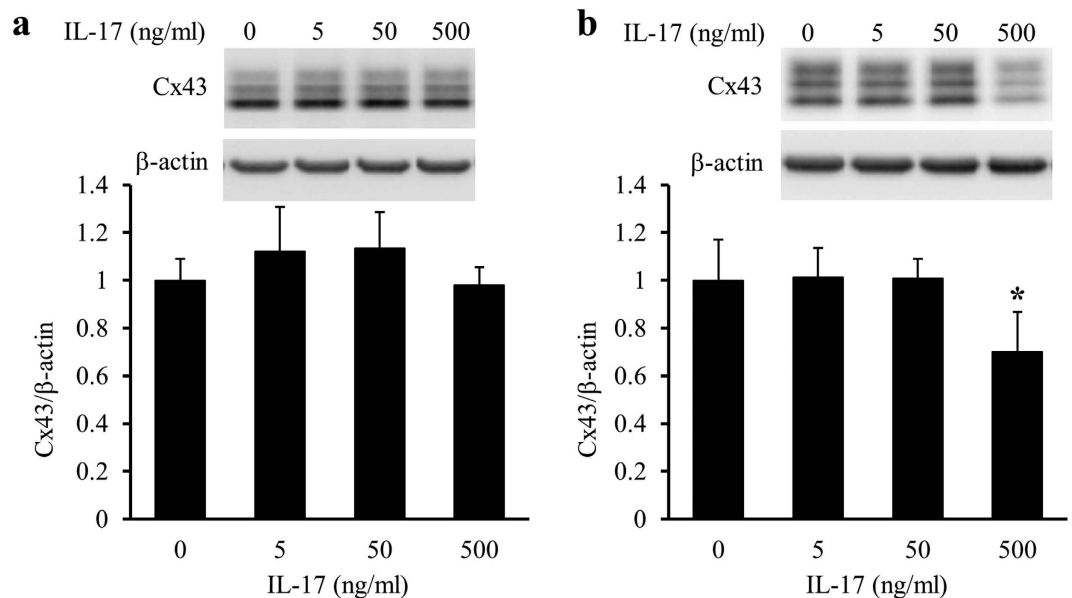


**Figure 3. Difference in the effects of IL-17 on Cx43 protein levels in the presence or absence of microglia in cultures.** Astrocyte-rich cultures (a) and astrocyte/microglia-mixed cultures (b) were treated with the vehicle (0) or 5, 50, and 500 ng/ml IL-17 for 24 h. Cx43 protein levels were assessed by western blotting.  $\beta$ -actin was used as a loading control. Cx43/ $\beta$ -actin of the vehicle treatment was set as 1. Data are presented as the mean  $\pm$  s.d. (n = 4, \* $p$  < 0.05, compared with the vehicle-treated control by one-way ANOVA followed by Dunnett's multiple comparison test). Full-length blots are presented in Supplementary Fig. S7.

protein levels in astrocytes ( $p = 0.0038$ ). These findings suggest that IFN $\gamma$  derived from Th1 cells activates microglia to release IL-1 $\beta$ , the main factor in the reduction of Cx43 protein levels in astrocytes.

## Discussion

In this study, we demonstrated that IFN $\gamma$  activated microglia to release IL-1 $\beta$  that reduced astrocytic Cx43 mRNA and protein levels, and functionally inhibited GJs in astrocytes. Although IL-1 $\beta$  secreted from microglia activated by IFN $\gamma$  appeared to be the main factor in the reduction of Cx43 in astrocytes, other proinflammatory cytokines in concert, such as TNF $\alpha$  and IL-6, also reduced Cx43. Significant downregulation of astrocytic Cx43 was also induced by humoral factors secreted from Th1 cells, particularly IFN $\gamma$ . Unexpectedly, high concentrations of IL-17 also diminished Cx43 protein levels in astrocytes, but only in the presence of microglia.

It was previously reported that functionally coupled astroglial cells determined by a dye injection method are decreased in astrocyte/microglia cocultures from newborn rat brains in the presence of 5% microglia following administration of either TNF $\alpha$ , IL-1 $\beta$ , or IFN $\gamma$ <sup>20</sup>. However, it was unclear which cytokines were mainly responsible for Cx43 down-modulation and whether these cytokines acted directly or indirectly on astrocytes. In the present study, we clearly demonstrated that IFN $\gamma$  indirectly decreased astrocytic Cx43 protein levels through activation of microglia and the subsequent release of IL-1 $\beta$ . Our findings are consistent with a previous study showing that humoral factors secreted from microglia activated by lipopolysaccharide (LPS) stimulation reduce Cx43 expression in astrocytes<sup>18</sup>. Although IL-1 $\beta$  and TNF $\alpha$  secreted from LPS-stimulated microglia have been reported to be the main factors that inhibit Cx43 expression and functions of GJs in astrocytes<sup>18</sup>, in our study, IL-1 $\beta$  alone decreased Cx43 protein levels and TNF $\alpha$  had no additional effect on the Cx43 protein reduction induced by IL-1 $\beta$  treatment. These data are in accordance with previous studies that reported IL-1 $\beta$  downregulates the expression of Cx43 in astrocyte-rich cultures<sup>21,22</sup>. However, our present data differ from previous reports regarding the effects of proinflammatory cytokines on glial cells<sup>23,24</sup>. Haghikia *et al.* reported that TNF $\alpha$  inhibits the function of GJs in astrocyte/microglia co-cultures containing 5% microglia derived from rat brain<sup>23</sup>. Zhang *et al.* reported that IFN $\gamma$  and TNF $\alpha$ , but not IL-1 $\beta$ , directly reduce Cx43 expression and suppress the function of GJs in newborn rat-derived spinal astrocyte cultures, in which microglia were removed by shaking off, and >95% of the remaining cells were positive for GFAP<sup>24</sup>. In accordance with a previous report<sup>25</sup>, we also found that the shaking-off method alone was insufficient to fully remove microglial cells, as determined by Iba-1 staining. Therefore, we believe that microglia should be isolated from mixed glial cell cultures using anti-CD11b antibody-conjugated magnetic beads to purify astrocytes maximally<sup>26,27</sup>, and that differences in microglial removal methods may be partly responsible for the discrepancy among studies. Differences in animal species, cell sources, and culture conditions might also be causes for the inconsistency, because astrocytes demonstrate inter-species and regional morphological, molecular, and physiological heterogeneity<sup>28,29</sup>.

Our study indicates that decreased Cx43 protein levels in astrocytes were in part attributable to a reduction of Cx43 mRNA transcription caused by IFN $\gamma$ -activated microglia. The detailed intracellular signalling pathway that regulates Cx43 expression remains to be elucidated in astrocytes. Recently, intracellular signalling pathways, including c-Jun N-terminal kinase (JNK), nuclear factor- $\kappa$ B (NF- $\kappa$ B), and phosphatidylinositol

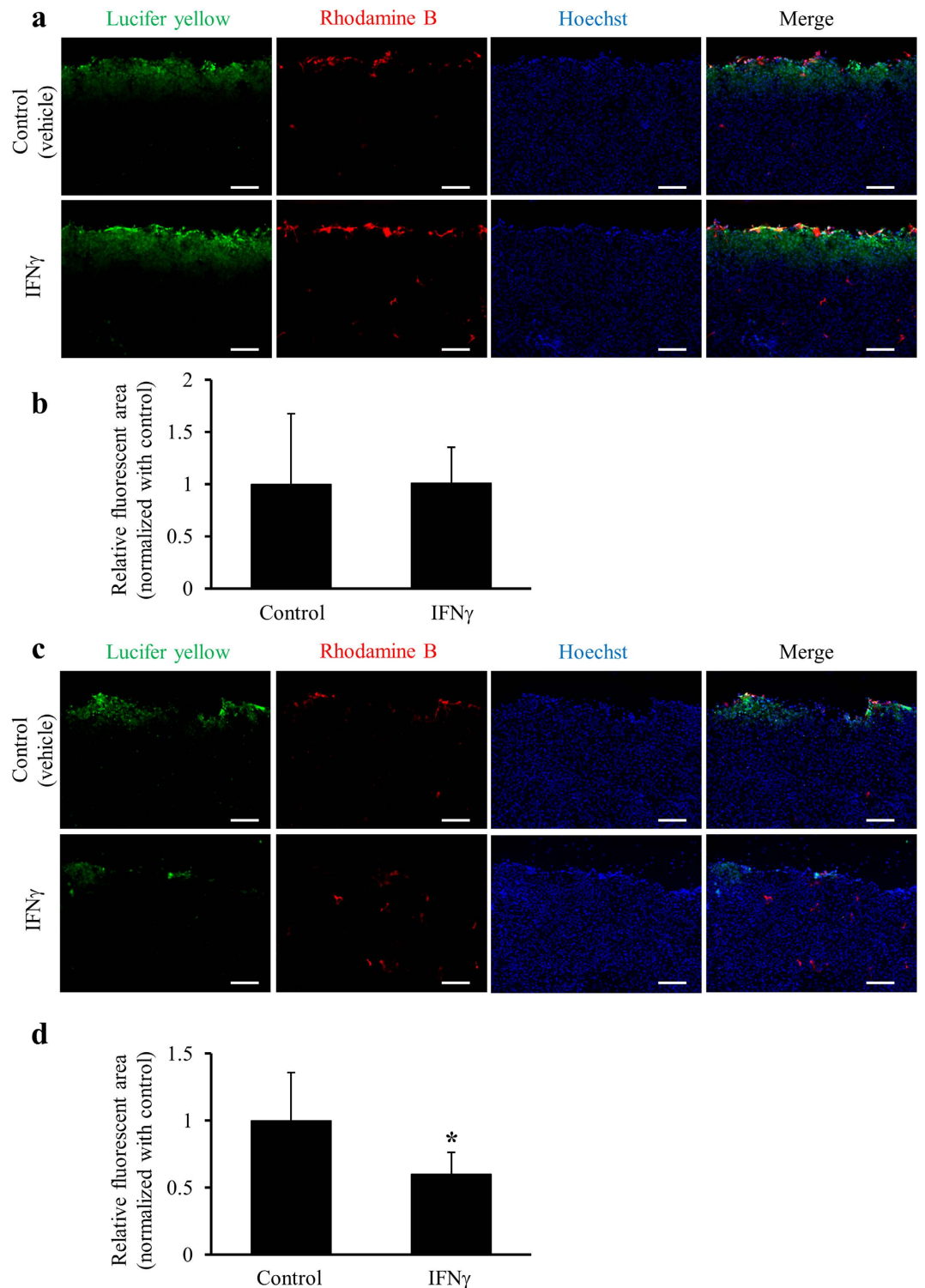


**Figure 4. Suppression of the function of GJs by treatment with IFN $\gamma$  in the presence or absence of microglia.** Confluent astrocyte-rich cultures (**a,b**) and confluent astrocyte/microglia-mixed cultures (**c,d**) were treated with the vehicle (control) or 500 ng/ml IFN $\gamma$  for 24 h. The functional states of GJs were measured by an SLDT assay as described in the Methods. (**a,c**) Representative micrographs show the distribution of Lucifer yellow (green) and Rhodamine B (red) in SLDT assays counterstained with Hoechst 33342 (blue). Scale bars: 500  $\mu$ m. (**b,d**) Graphs show quantitative data of the dye-spreading areas (rhodamine B-positive areas were subtracted from Lucifer yellow-positive areas) expressed as relative to those in controls (vehicle treatment). Data are presented as the mean  $\pm$  s.d. (two to three spots per well,  $n = 4$  wells per treatment). \* $p < 0.05$ , one-way ANOVA followed by Dunnett's multiple comparison test.

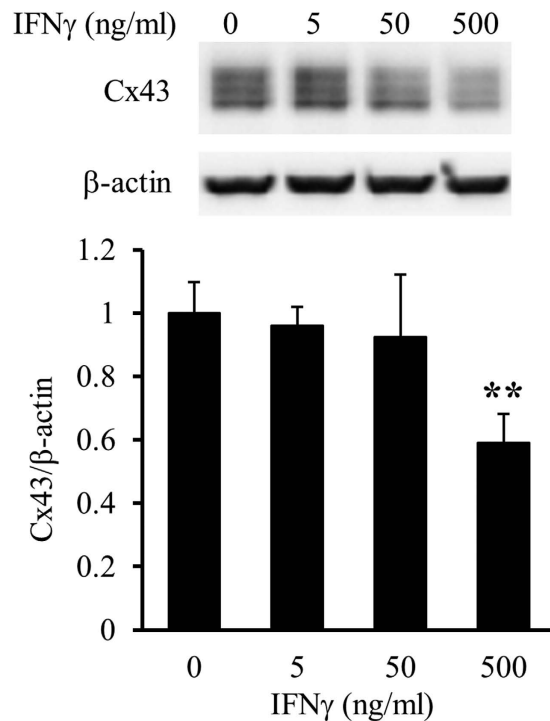


**Figure 5. Downregulation of Cx43 protein levels by IFN $\gamma$ -treated microglia-conditioned media in astrocyte-rich cultures.** Isolated microglia were treated with the vehicle (0) or 5, 50, and 500 ng/ml IFN $\gamma$  for 24 h. IFN $\gamma$ -treated microglia-conditioned media were collected and used to treat astrocyte-rich cultures for 24 h. Cx43 protein levels were assessed by western blotting.  $\beta$ -actin was used as the loading control. Cx43/ $\beta$ -actin of control (vehicle-treated microglia conditioned medium) was set as 1. Data are presented as the mean  $\pm$  s.d. ( $n = 4$ ,  $**p < 0.01$ , compared with the vehicle-treated control by one-way ANOVA followed by Dunnett's multiple comparison test). Full-length blots are presented in Supplementary Fig. S8.

3-kinase, were reported to regulate the expression of Cx43 in astrocytes<sup>24,30,31</sup>. In addition, the JNK-dependent ubiquitin-proteasome system was reported to be involved in regulating the protein levels of Cx43 through degradation<sup>31,32</sup>. Because IL-1 $\beta$  activates JNK and NF- $\kappa$ B pathways in astrocytes<sup>33</sup>, the decrease in Cx43 protein levels might be partly caused by a reduction in Cx43 mRNA transcription through JNK and NF- $\kappa$ B pathways and increased degradation by activation of the JNK pathway via IL-1 $\beta$  secreted from IFN $\gamma$ -activated microglia.

We and others have reported significant increases in IFN $\gamma$ -producing T cells in the cerebrospinal fluid (CSF) of MS patients, and the presence of IFN $\gamma$ -positive lymphocytes in MS lesions<sup>34–36</sup>. Notably, IFN $\gamma$  injection causes MS relapses<sup>37</sup>. IFN $\gamma$  production also correlates with exacerbation of neurological symptoms<sup>38</sup>. These findings indicate active involvement of IFN $\gamma$ -producing Th1 cells in MS. However, the mechanisms of how these Th1 cells contribute to demyelinating lesion formation are not completely resolved. How huge demyelinating lesions occasionally develop despite the presence of perivascular inflammatory cell infiltration occurring in limited areas around vessels is also unclear. We previously reported extensive loss of Cx43 in MS and NMO lesions, and that cases with extensive Cx43 loss more frequently have a malignant course culminating in death within 2 years after disease onset<sup>11</sup>. It is notable that astrocytic Cx43 expression is lost at the leading edges of concentric lesions in BCS patients, where myelin and myelin proteins are preserved, including oligodendrocytic Cx32 and Cx47<sup>10</sup>. In EAE induced by myelin oligodendrocyte glycoprotein or myelin basic protein, diffuse loss of glial Cxs, such as Cx32, Cx43, and Cx47, occurs in acute lesions<sup>39,40</sup>. Based on these observations, we propose that early loss of astrocytic Cx43 may lead to the formation of extensive demyelinating lesions. This notion is supported by the fact that astrocytic Cx43/Cx30 double-knockout mice show widespread white matter pathologies including vacuolated oligodendrocytes, intramyelinic oedema, loss of mature oligodendrocytes, and increased numbers of apoptotic cells<sup>41</sup>.

Astrocytes form glial syncytia by coupling to adjacent astrocytes and oligodendrocytes via Cx43 GJs. This process maintains homeostasis of the CNS<sup>4</sup>. Therefore, early loss of astrocytic Cx43 may promote oligodendrocyte apoptosis by disrupting glial syncytia, resulting in secondary demyelination. Furthermore, the absence of astroglial Cx43/Cx30 weakens blood-brain barrier integrity<sup>42</sup>. Intriguingly, Boulay *et al.* recently reported that astroglial Cx43 controls immune cell recruitment<sup>43</sup>. Thus, downregulation of astrocytic Cx43 may promote infiltration of immune cells into brain parenchyma and propagate inflammatory reactions, especially in the presence of proinflammatory cytokines and chemokines produced by activated microglia, as shown by the current and previous studies<sup>44,45</sup>. Taken together, IFN $\gamma$ -dominant inflammatory states might disrupt astrocytic intercellular communication, which can lead to exacerbation of inflammation and extensive demyelination.



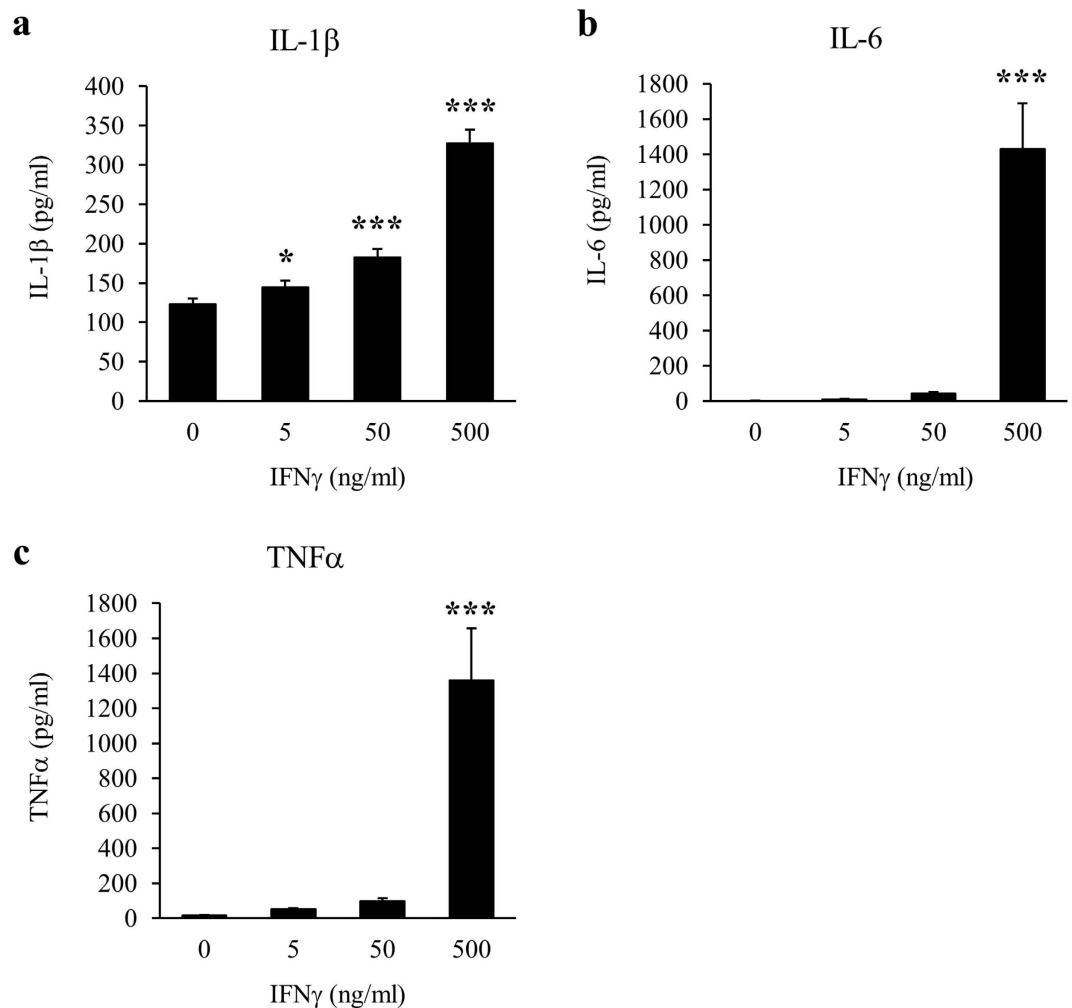


**Figure 6. Proinflammatory cytokine concentrations in IFN $\gamma$ -treated microglia-conditioned media.**

Isolated microglia were treated with the vehicle (0) or 5, 50, and 500 ng/ml IFN $\gamma$  for 24 h. IFN $\gamma$ -treated microglia-conditioned media were collected and several cytokine concentrations were measured using the Bio-Plex Multiplex System. The expression levels of (a) IL-1 $\beta$ , (b) IL-6, and (c) TNF $\alpha$  are shown in each graph. Data are presented as the mean  $\pm$  s.d. (n = 4, \* $p$  < 0.05, \*\* $p$  < 0.01, and \*\*\* $p$  < 0.001, compared with the vehicle-treated control by one-way ANOVA followed by Dunnett's multiple comparison test).

In terms of IL-17, *IL17* mRNA expression, the frequency of Th17 cells, and IL-17 levels increase in the blood and CSF of MS patients<sup>46–48</sup>. Th17 cells are enriched in MS lesions<sup>49</sup>, and both Th17 cells and IL-17 have a pivotal role in the pathogenesis of EAE<sup>50,51</sup>. It is interesting that high IL-17 concentrations downregulated the Cx43 protein levels of astrocytes in coculture with microglia in our study. Thus, Th17 cells may also contribute to Cx43 loss in the brain parenchyma where astrocytes and microglia may be exposed to high concentrations of IL-17 when in the close contact with infiltrated Th17 cells.

It was recently reported that two-thirds of CNS-infiltrating Th17 cells express IFN $\gamma$  in EAE<sup>52,53</sup>, and that T cells secreting IL-17 alone or IL-17 and IFN $\gamma$  infiltrate the CNS prior to the onset of clinical symptoms of EAE, where they may mediate CNS inflammation through microglial activation<sup>54</sup>. It was also reported that IL-17<sup>+</sup> IFN $\gamma$ <sup>+</sup> CD4<sup>+</sup> T cells are abundant in MS lesions<sup>55</sup>. These IL-17 and IFN $\gamma$  double-positive cells are regarded as pathogenic Th17 cells that develop under a Th1-prone cytokine milieu and become ex-Th17 cells producing IFN $\gamma$  but not IL-17<sup>56,57</sup>. Therefore, Th17 cells may also contribute to MS lesion formation via IFN $\gamma$  that effectively reduces Cx43 expression in astrocytes.

In conclusion, we propose that Th1 cell-derived humoral factors, mainly IFN $\gamma$ , induce microglial activation and the release of IL-1 $\beta$  that downregulates astrocytic Cx43, which might exacerbate the inflammatory processes in demyelinating disorders. Thus, IFN $\gamma$  and Th1-prone conditions are important targets to prevent development of extensive demyelinating lesions.

## Methods

**Animals.** All cultures were prepared using cells from C57BL/6 J mice (Charles River Laboratories Japan, Inc., Yokohama, Japan). The protocols for animal experiments were reviewed and approved by the Committee of

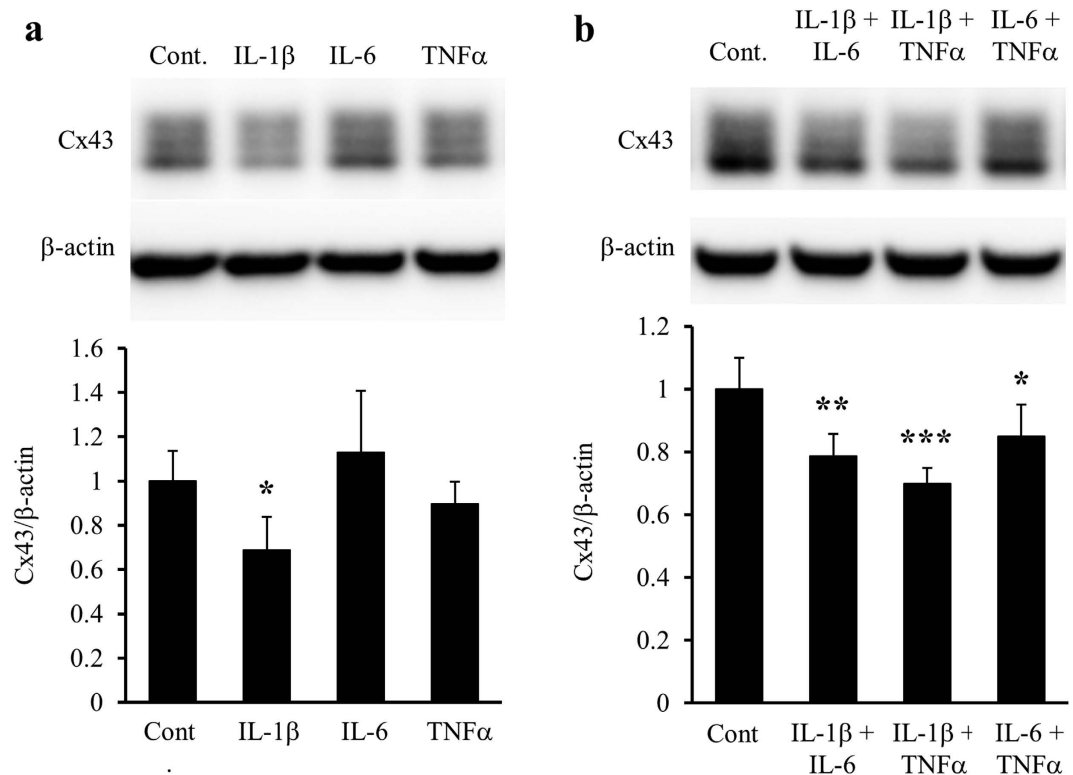


**Figure 7. Effects of IL-1 $\beta$ , IL-6, and TNF $\alpha$  on Cx43 protein levels in astrocyte-rich cultures.** Astrocyte-rich cultures were treated with 300 pg/ml IL-1 $\beta$ , 1400 pg/ml IL-6, or 1300 pg/ml TNF $\alpha$  alone (a) or in combinations (b) for 24 h. Cx43 protein levels were evaluated by western blotting.  $\beta$ -actin was used as a loading control. Cx43/ $\beta$ -actin of vehicle treatment (control, shown as “Cont.”) was set as 1. Data are presented as the mean  $\pm$  s.d. (n = 5, \* $p$  < 0.05, \*\* $p$  < 0.01, and \*\*\* $p$  < 0.001, compared with the control by one-way ANOVA followed by Dunnett’s multiple comparison test). Full-length blots are presented in Supplementary Fig. S8.

Ethics on Animal Experiments at Kyushu University Faculty of Medicine (A25–196, A27–205). All animal experiments were performed in accordance with the Regulations for Animal Experiments defined by the Institutional Animal Care and Use Committee at Kyushu University.

**Glial cell cultures.** Primary mixed glial cell cultures were prepared from the brains of newborn C57BL/6 J mice according to a previously described method<sup>58</sup>. Briefly, brains were removed under sterile conditions, and the meninges were carefully removed. The tissue was dissociated by passing through a nylon mesh in Hanks’ balanced salt solution (HBSS; Sigma-Aldrich, Saint Louis, MO, USA) containing 50 U/ml penicillin and 50  $\mu$ g/ml streptomycin (Gibco, Thermo Fisher Scientific, Waltham, MA, USA) to prevent contamination. After washing with HBSS, the cell suspension was plated in 75 cm<sup>2</sup> culture flasks at a density of one to two brains per flask in 10 ml of GM. GM consisted of Dulbecco’s Modified Eagle’s Medium (Sigma-Aldrich) supplemented with 10% fetal bovine serum (FBS) (Equitech-Bio, Kerrville, TX, USA), 5  $\mu$ g/ml bovine insulin (Sigma-Aldrich), and 0.2% glucose. The cells were maintained at 37 °C in a humidified atmosphere containing 5% CO<sub>2</sub> with three medium changes in the first week and no medium change in the second week to induce the proliferation of microglia. At confluency (12–15 days), mixed glial cells were detached by Accutase (Innovative Cell Technologies, San Diego, CA, USA) treatment and replated. After 5–10 days of culture, mixed glial cell cultures that had reached 100% confluence were used for experiments.

We also generated astrocyte-rich cultures and microglial cultures from primary mixed glial cell cultures using magnetic-activated cell sorting (MACS, Miltenyi Biotec, Bergisch Gladbach, Germany). Mixed glial cell cultures were prepared as described above, and glial cells were detached by Accutase treatment at day 12–15. The cell suspension was washed and resuspended in 10 ml MACS Separation Buffer (Miltenyi Biotec). After filtration through a 70  $\mu$ m pore filter, the cell suspension was centrifuged at 300  $\times$  g for 5 min at 4 °C. Then, the cells were separated into CD11b-positive and -negative fractions using CD11b MicroBeads (microbeads conjugated to a monoclonal rat anti-mouse CD11b Ab; Miltenyi Biotec) according to the manufacturer’s protocol with some modification<sup>26,27</sup>. Briefly, 1  $\times$  10<sup>7</sup> cells were resuspended in 90  $\mu$ l of separation buffer and 10  $\mu$ l of CD11b MicroBeads, and incubated at 4 °C for 30 min with gentle mixing every 10 min. Then, the cells were washed and resuspended in 500  $\mu$ l of separation buffer per 1  $\times$  10<sup>8</sup> cells. The cell suspension was applied to an LS column (Miltenyi Biotec) fitted into the QuadroMACS™ cell separator (Miltenyi Biotec), and then the cells were separated into CD11b-negative and -positive fractions. The astrocyte-enriched fraction (astrocyte-rich culture), corresponding to the CD11b-negative fraction, was resuspended in GM before plating. After 7–10 days,

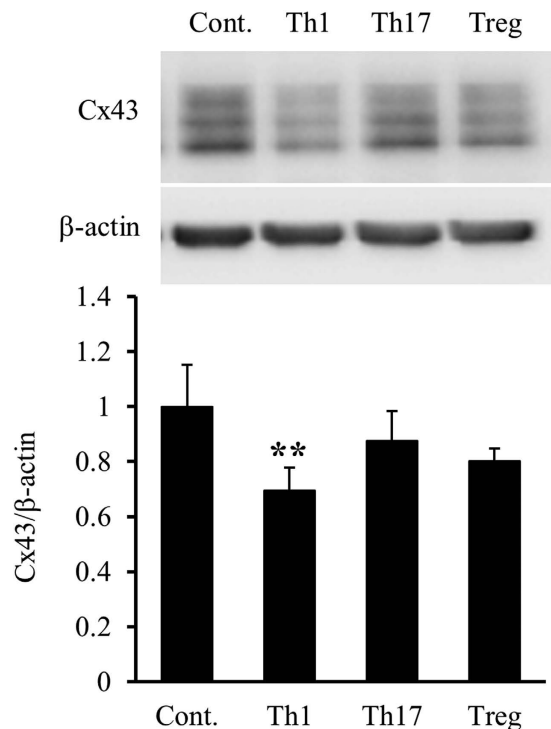


**Figure 8. Reduction of Cx43 protein levels in astrocytes induced by the Th1 cell culture supernatant.**

Mixed glial cell cultures were treated with conditioned media of Th1, Th17, and Treg cells for 24 h. Cx43 protein levels were evaluated by western blotting.  $\beta$ -actin was used as a loading control. Cx43/ $\beta$ -actin of mixed glial cells without treatment (control, shown as “Cont.”) was set as 1. Data are presented as the mean  $\pm$  s.d. ( $n = 4$ ,  $**p < 0.01$ , compared with the control by one-way ANOVA followed by Dunnett’s multiple comparison test). Full-length blots are presented in Supplementary Fig. S9.

astrocyte-rich cultures that reached 100% confluence were used for experiments. The CD11b-positive fraction containing microglia was plated in GM and used for experiments after 24 h (microglial culture). CD11b-negative and -positive fractions were mixed at a ratio of 3:1 (astrocyte/microglia-mixed culture). After 7–10 days, mixed cultures that reached 100% confluence were used for experiments.

**Helper T cell differentiation.** Spleens were aseptically removed from C57BL/6 J mice (8–10 weeks old), and splenocytes were dissociated into single cells. After red blood cell lysis, naive  $CD4^+$  T cells were isolated from the splenocytes using a Naive  $CD4^+$  T Cell Isolation Kit (Miltenyi Biotec) according to the manufacturer’s protocol and suspended in complete RPMI medium [RPMI-1640 medium supplemented with 2 mM L-glutamine (Sigma-Aldrich), 1 mM sodium pyruvate (Gibco, Thermo Fisher Scientific), 50  $\mu$ M 2-mercaptoethanol, 50 U/ml penicillin, 50  $\mu$ g/ml streptomycin, and 10% FBS (Cell Culture Bioscience, Lenexa, KS, USA)]. Purified naive  $CD4^+$  T cells ( $1 \times 10^5$  cells/well) were seeded in 96-well plates pre-coated with 5  $\mu$ g/ml anti-CD3e Ab. The cells were cultured under Th1 (20 ng/ml IL-2, 20 ng/ml IL-12, and 10  $\mu$ g/ml anti-IL-4 Ab), Th17 [5 ng/ml transforming growth factor (TGF)  $\beta$ , 30 ng/ml IL-6, and 10  $\mu$ g/ml anti-IFN $\gamma$  Ab], or Treg (5 ng/ml TGF $\beta$  and 20 ng/ml IL-2)-skewing conditions in 200  $\mu$ l of complete RPMI medium with 2  $\mu$ g/ml anti-CD28 Ab for 3 days. On day 3, differentiated T cells were collected and washed with complete RPMI medium. Then, the cells were resuspended in complete RPMI medium at  $5 \times 10^5$  cells/ml and reseeded with 2  $\mu$ g/ml anti-CD28 Ab in 96-well plates pre-coated with anti-CD3e Ab for 24 h. On day 4, the T cell culture supernatants were collected and stored at  $-80^\circ\text{C}$  before being used for treatment of glial cells. Recombinant mouse IL-2, IL-12, and TGF $\beta$  were purchased from R&D Systems (Minneapolis, MN, USA). Recombinant mouse IL-6 was purchased from BioLegend (San Diego, CA, USA). No azide/low endotoxin-grade anti-IL-4 (clone 11B11, rat IgG $_1$ ), anti-IFN $\gamma$  (clone XMG1.2, rat IgG $_1$ ), anti-CD3e (clone 145-2C11, hamster IgG $_1$ ), and anti-CD28 (clone 37.51, hamster IgG $_2$ ) Abs were purchased from BD Biosciences (Franklin Lakes, NJ, USA).

The purity and differentiation state of naive  $CD4^+$  T cells and differentiated T cells were confirmed by flow cytometry. Before staining, Th1 and Th17 cells were stimulated with 25 ng/ml phorbol 12-myristate 13-acetate (Sigma-Aldrich) and 1  $\mu$ g/ml ionomycin (Sigma-Aldrich) for 5 h, and 10  $\mu$ g/ml brefeldin A (Sigma-Aldrich) was added for the last 4 h. T cells were washed and blocked with an anti-CD16/32 Ab. Naive  $CD4^+$  T cells were stained with anti-CD4 (clone RM4-5), anti-I-A/I-E, anti-CD44, and anti-CD62L Abs. Th1 and Th17 cells were stained with anti-CD4 (clone RM4-5) and anti-I-A/I-E Abs. Treg cells were stained with anti-CD4 (clone GK1.5), anti-I-A/I-E, and anti-CD25 Abs. Differentiated T cells were fixed and permeabilized with Fixation buffer and Permeabilization Wash Buffer (Sony Biotechnology, Champaign, IL, USA) for Th1 and Th17 cells or FOXP3 Fix/Perm buffer Set (Sony Biotechnology) for Treg cells, and then stained intracellularly (anti-IFN $\gamma$ , anti-IL-4, and

anti-IL-17A Abs for Th1 and Th17 cells; anti-mouse/rat Foxp3 Ab for Treg cells). The cells were subsequently analysed by flow cytometry using a Cell Sorter SH-800 (Sony, Tokyo, Japan). Detailed information of the Abs used in flow cytometry is listed in Supplementary Table S1.

The purity of naïve CD4<sup>+</sup> T cells (CD44<sup>lo</sup>CD62<sup>+</sup> cells) was typically 93% or higher. Differentiated Th1 and Th17 cells predominantly expressed IFN $\gamma$  and IL-17, respectively, but rarely expressed IL-4. Most Treg cells expressed both CD25 and Foxp3 (Supplementary Fig. S5).

**Treatment of glial cells.** Mixed glial cell cultures, astrocyte-rich cultures, and astrocyte/microglia-mixed cultures were treated with recombinant mouse IFN $\gamma$ , IL-4, and IL-17 (R&D Systems) diluted in GM for 24 h. Astrocyte-rich cultures were treated with recombinant mouse IL-1 $\beta$ , IL-6 (BioLegend), and TNF $\alpha$  (R&D Systems) diluted in GM for 24 h. The concentrations of these cytokines were 300 pg/ml for IL-1 $\beta$ , 1400 pg/ml for IL-6, and 1300 pg/ml for TNF $\alpha$  based on their concentrations in IFN $\gamma$ -treated microglia-conditioned medium. Astrocyte-rich cultures were also treated with 0, 180, 240 or 300 pg/ml recombinant mouse IL-1 $\beta$  for 24 h. The concentrations of IL-1 $\beta$  at 180 and 300 pg/ml were approximately equal to those of IL-1 $\beta$  in microglia-conditioned media when microglia were treated with 50 or 500 ng/ml IFN $\gamma$  for 24 h, respectively. Upon treatment of mixed glial cells with conditioned media from T cells, they were diluted in GM at a ratio of 1:1, and treatments were performed for 24 h.

**Western blotting of Cx43.** After all treatments of glial cells, the cells were solubilised in a radioimmunoprecipitation assay buffer containing a protease inhibitor cocktail, 0.5% sodium dodecyl sulfate (Nacalai Tesque, Kyoto, Japan), and PhosSTOP phosphatase inhibitor cocktail (Roche Diagnostics, Mannheim, Germany). The lysates were placed on ice for 30 min and then centrifuged at 4 °C for 10 min at 10,000  $\times$  g. Supernatants were collected, analysed for protein concentrations using a BCA protein assay kit (Pierce, Thermo Fisher Scientific), and adjusted to equal protein concentrations. Laemmli's buffer was added to the protein samples, followed by boiling at 95 °C for 5 min. Equal amounts of protein were separated by 7.5–15% gradient poly-acrylamide gel (REAL GEL PLATE, Bio Craft, Tokyo, Japan) electrophoresis and blotted onto polyvinylidene difluoride membranes. The membranes were incubated with a blocking solution [Blocking One-P for Cx43 and Blocking One (Nacalai Tesque) for  $\beta$ -actin] and subsequently incubated with an anti-Cx43 Ab (1:10,000; rabbit polyclonal IgG; Abcam, Cambridge, UK) overnight at 4 °C or with an anti- $\beta$ -actin Ab (1:20,000; clone AC-15, mouse monoclonal IgG1; Sigma-Aldrich) for 1 h at room temperature. After washing, the membranes were incubated with a horseradish peroxidase-conjugated secondary Ab for 1 h at room temperature. Then, the membranes were washed and visualized by enhanced chemiluminescence (ECL Prime, GE Healthcare Bio-Sciences AB, Uppsala, Sweden). Band intensities were measured using the ChemiDoc<sup>TM</sup> XRS system (Bio-Rad Laboratories, Hercules, CA, USA) and normalized to  $\beta$ -actin levels.

**Immunocytochemistry.** Glial cells plated on collagen type 1-coated 8-well culture slides (Corning, Corning, NY, USA) were washed with PBS, fixed with 4% paraformaldehyde for 5 min, and permeabilised with 0.05% Triton X-100 in PBS (PBS-T) for 15 min. The cells were incubated with primary Abs against Cx43, Iba-1, GFAP, NeuN, Nogo-A, or NG2 (detailed information of Abs are listed in Supplementary Table S2) in PBS-T with 5% goat serum for 1 h at 37 °C. After rinsing, the cells were incubated with Alexa 488- and 546- or 594-conjugated secondary Abs and 4',6-diamidino-2-phenylindole (DAPI) for 30 min at 37 °C. Images were captured using a confocal laser microscope system (Nikon A1, Nikon, Tokyo, Japan) with Plan-Apochromat 20  $\times$  (0.75 NA) or Plan-Apochromat 10  $\times$  (0.45 NA) objective (Nikon) or fluorescence microscope (BZ-X700, Keyence, Osaka, Japan) with Plan-Apochromat 20  $\times$  (0.75 NA) or Plan-Fluor 10  $\times$  (0.30 NA) objective (Nikon).

**RNA extraction and quantitative real-time reverse transcriptase (RT)-PCR.** Total RNA was extracted from cells using an RNeasy Mini kit (Qiagen, Venlo, Netherlands) following the manufacturer's instructions. cDNA was synthesized using ReverTra Ace qPCR RT Master Mix with gDNA Remover (Toyobo, Osaka, Japan). Quantitative real-time RT-PCR analysis of cDNAs was performed with an Applied Biosystems 7500 Real-Time PCR System (Applied Biosystems, Thermo Fisher Scientific) using TaqMan Gene Expression Master Mix and TaqMan Gene Expression Assays (Cx43 (*Gja1*), Mm01179639\_s1; Gapdh, Mm99999915\_g1; Applied Biosystems, Thermo Fisher Scientific). Gapdh was used as an internal control gene. PCR cycling conditions were 50 °C for 2 min, 95 °C for 10 min, followed by 40 cycles of 95 °C for 15 sec and 60 °C for 1 min. The  $\Delta\Delta$ CT efficiency corrected method was used to calculate relative mRNA levels.

**SLDT Assay.** GJ permeability was determined at 37 °C using a SLDT assay as described previously<sup>59</sup> with minor modifications. In brief, confluent glial cells in 12-well plates were washed with PBS and scraped in the presence of PBS containing 0.1% of the fluorescent dye Lucifer yellow (molecular weight: 457.3 Da; Sigma-Aldrich) and 0.05% rhodamine B-dextran (molecular weight: 10,000 Da; Molecular Probes, Thermo Fisher Scientific). After 2 min of incubation, the cells were washed three times with PBS and then incubated for an additional 5 min in PBS to allow the loaded dye to transfer to adjoining cells. The cells were then fixed with 4% paraformaldehyde, counterstained with Hoechst 33342, and observed under a fluorescence microscope. Damaged cells absorb the dye mixture and transfer Lucifer yellow into neighbouring cells through functional GJs. In contrast, rhodamine B-dextran does not pass through GJ and is restricted to the initially loaded cells. Dye diffusion was captured using fluorescence microscope (BZ-X700, Keyence) with Plan-Fluor 10  $\times$  (0.30 NA) objective (Nikon), and quantified by measuring fluorescent areas. Quantification of the function of GJs was performed by subtraction of the rhodamine B-positive fluorescent area from the Lucifer yellow-positive fluorescent area by ImageJ software (US National Institutes of Health, Bethesda, MD, USA).

**ELISA.** The levels of IFN $\gamma$  in culture supernatants were measured by an ELISA kit (Quantikine<sup>®</sup> ELISA Mouse IFN- $\gamma$  Immunoassay; R&D systems) according to the manufacturer's instructions.

**Multiplexed fluorescent bead-based immunoassay.** IFN $\gamma$ -treated microglia-conditioned media were collected and analysed simultaneously for 23 cytokines and chemokines: IL-1 $\alpha$ , IL-1 $\beta$ , IL-2, IL-3, IL-4, IL-5, IL-6, IL-9, IL-10, IL-12 (p40), IL-12 (p70), IL-13, IL-17A, TNF $\alpha$ , granulocyte-colony stimulating factor, granulocyte-macrophage colony-stimulating factor, IFN $\gamma$ , chemokine (C-X-C motif) ligand 1 (KC), chemokine (C-C motif) ligand (CCL) 2 (monocyte chemoattractant protein 1), CCL3 [Macrophage inflammatory protein (MIP)-1 $\alpha$ ], CCL4 (MIP-1 $\beta$ ), CCL5 (RANTES), and CCL11 (eotaxin) by a Bio-Plex Multiplex System (Bio-Rad Laboratories) according to the manufacturer's instructions<sup>36</sup>. All samples were analysed undiluted in duplicate.

**Statistical analysis.** Data are expressed as the mean  $\pm$  standard deviation (s.d.) of at least four experiments. One-way analysis of variance (ANOVA) followed by a Dunnett's multiple comparison test were used to analyse data. All analyses were carried out using JMP<sup>®</sup> Pro version 11.0.0 software (SAS Institute, Cary, NC, USA). The significance level was set at  $p < 0.05$ .

## References

1. Massa, P. T. & Mugnaini, E. Cell junctions and intramembrane particles of astrocytes and oligodendrocytes: a freeze-fracture study. *Neuroscience*. **7**, 523–538 (1982).
2. Rash, J. E., Yasumura, T., Dudek, F. E. & Nagy, J. I. Cell specific expression of connexins and evidence of restricted gap junctional coupling between glial cells and between neurons. *J. Neurosci.* **21**, 1983–2000 (2001).
3. Takeuchi, H. & Suzumura, A. Gap junctions and hemichannels composed of connexins: potential therapeutic targets for neurodegenerative diseases. *Front. Cell. Neurosci.* **8**, 189 (2014).
4. Orthmann-Murphy, J. L., Abrams, C. K. & Scherer, S. S. Gap junctions couple astrocytes and oligodendrocytes. *J. Mol. Neurosci.* **35**, 101–116 (2008).
5. Dermietzel, R., Hertzberg, E. L., Kessler, J. A. & Spray, D. C. Gap junctions between cultured astrocytes: immunocytochemical, molecular, and electrophysiological analysis. *J. Neurosci.* **11**, 1421–1432 (1991).
6. Giaume, C. *et al.* Gap junctions in cultured astrocytes: single-channel currents and characterization of channel-forming protein. *Neuron*. **6**, 133–143 (1991).
7. Yamamoto, T., Ochalski, A., Hertzberg, E. L. & Nagy, J. I. LM and EM immunolocalization of the gap junctional protein connexin 43 in rat brain. *Brain Res.* **508**, 313–319 (1990).
8. Simard, M., Arcuino, G., Takano, T., Liu, Q. S. & Nedergaard, M. Signaling at the gliovascular interface. *J. Neurosci.* **23**, 9254–9262 (2003).
9. Altevogt, B. M. & Paul, D. L. Four classes of intercellular channels between glial cells in the CNS. *J. Neurosci.* **24**, 4313–4323 (2004).
10. Masaki, K. *et al.* Extensive loss of connexins in Baló's disease: evidence for an auto-antibody-independent astrocytopathy via impaired astrocyteoligodendrocyte/myelin interaction. *Acta Neuropathol.* **123**, 887–900 (2012).
11. Masaki, K. *et al.* Connexin 43 astrocytopathy linked to rapidly progressive multiple sclerosis and neuromyelitis optica. *PLoS One*. **8**, e72919 (2013).
12. Masaki, K. Connexin pathology in acute multiple sclerosis, Baló's disease and neuromyelitis optica. *Clin. Exp. Neuroimmunol.* **4**, 36–44 (2013).
13. Kira, J. Autoimmunity in neuromyelitis optica and opticospinal multiple sclerosis: astrocytopathy as a common denominator in demyelinating disorders. *J. Neurol. Sci.* **311**, 69–77 (2011).
14. Masaki, K. Early disruption of glial communication via connexin gap junction in multiple sclerosis, Baló's disease and neuromyelitis optica. *Neuropathology*. **35**, 469–480 (2015).
15. Orellana, J. A., Martinez, A. D. & Retamal, M. A. Gap junction channels and hemichannels in the CNS: regulation by signaling molecules. *Neuropharmacology*. **75**, 567–582 (2013).
16. Sospedra, M. & Martin, R. Immunology of multiple sclerosis. *Annu. Rev. Immunol.* **23**, 683–747 (2005).
17. Aloisi, F. Immune function of microglia. *Glia*. **36**, 165–179 (2001).
18. Mème, W. *et al.* Proinflammatory cytokines released from microglia inhibit gap junctions in astrocytes: potentiation by  $\beta$ -amyloid. *FASEB J.* **20**, 494–496 (2006).
19. Franco, R. & Fernández-Suárez, D. Alternatively activated microglia and macrophages in the central nervous system. *Prog. Neurobiol.* **131**, 65–86 (2015).
20. Hinkerohe, D. *et al.* Effects of cytokines on microglial phenotypes and astroglial coupling in an inflammatory coculture model. *Glia*. **52**, 85–97 (2005).
21. John, G. R. *et al.* IL-1 $\beta$  differentially regulates calcium wave propagation between primary human fetal astrocytes via pathways involving P2 receptors and gap junction channels. *Proc. Natl. Acad. Sci. USA* **96**, 11613–11618 (1999).
22. Zeis, T. *et al.* Metabolic gene expression changes in astrocytes in Multiple Sclerosis cerebral cortex are indicative of immune-mediated signaling. *Brain Behav. Immun.* **48**, 313–325 (2015).
23. Haghikia, A. *et al.* Intracellular application of TNF-alpha impairs cell to cell communication via gap junctions in glioma cells. *J. Neurooncol.* **86**, 143–152 (2008).
24. Zhang, F. F., Morioka, N., Nakashima-Hisaoka, K. & Nakata, Y. Spinal astrocytes stimulated by tumor necrosis factor- $\alpha$  and/or interferon- $\gamma$  attenuate connexin 43-gap junction via c-jun terminal kinase activity. *J. Neurosci. Res.* **91**, 745–756 (2013).
25. Saura, J. Microglial cells in astroglial cultures: a cautionary note. *J. Neuroinflammation*. **4**, 26 (2007).
26. Marek, R., Caruso, M., Rostami, A., Grinspan, J. B. & Das Sarma, J. Magnetic cell sorting: a fast and effective method of concurrent isolation of high purity viable astrocytes and microglia from neonatal mouse brain tissue. *J. Neurosci. Methods*. **175**, 108–118 (2008).
27. Losciuto, S. *et al.* An efficient method to limit microglia-dependent effects in astroglial cultures. *J. Neurosci. Methods*. **207**, 59–71 (2012).
28. Oberheim, N. A., Goldman, S. A. & Nedergaard, M. Heterogeneity of astrocytic form and function. *Methods Mol. Biol.* **814**, 23–45 (2012).
29. Theis, M. & Giaume, C. Connexin-based intercellular communication and astrocyte heterogeneity. *Brain Res.* **1487**, 88–98 (2012).
30. Zhao, Y., Rivieccio, M. A., Lutz, S., Scemes, E. & Brosnan, C. F. The TLR3 ligand polyI: C downregulates connexin 43 expression and function in astrocytes by a mechanism involving the NF- $\kappa$ B and PI3 kinase pathways. *Glia*. **54**, 775–785 (2006).
31. Liao, C. K., Jeng, C. J., Wang, H. S., Wang, S. H. & Wu, J. C. Lipopolysaccharide induces degradation of connexin43 in rat astrocytes via the ubiquitin-proteasome proteolytic pathway. *PLoS One*. **8**, e79350 (2013).
32. Zhang, F. F., Morioka, N., Kitamura, T., Hisaoka-Nakashima, K. & Nakata, Y. Proinflammatory cytokines downregulate connexin 43-gap junctions via the ubiquitin-proteasome system in rat spinal astrocytes. *Biochem. Biophys. Res. Commun.* **464**, 1202–1208 (2015).



33. Wu, C. Y., Hsieh, H. L., Jou, M. J. & Yang, C. M. Involvement of p42/p44 MAPK, p38 MAPK, JNK and nuclear factor-kappa B in interleukin-1 $\beta$ -induced matrix metalloproteinase-9 expression in rat brain astrocytes. *J. Neurochem.* **90**, 1477–1488 (2004).
34. Traugott, U. & Lebon, P. Multiple sclerosis: involvement of interferons in lesion pathogenesis. *Ann. Neurol.* **24**, 243–251 (1988).
35. Olsson, T. *et al.* Autoreactive T lymphocytes in multiple sclerosis determined by antigen-induced secretion of interferon-gamma. *J. Clin. Invest.* **86**, 981–985 (1990).
36. Ishizu, T. *et al.* Intrathecal activation of the IL-17/IL-8 axis in opticospinal multiple sclerosis. *Brain.* **128**, 988–1002 (2005).
37. Panitch, H. S., Hirsch, R. L., Haley, A. S. & Johnson, K. P. Exacerbations of multiple sclerosis in patients treated with gamma interferon. *Lancet.* **329**, 893–895 (1987).
38. Petereit, H. F., Richter, N., Pukrop, R. & Bamborschke, S. Interferon gamma production in blood lymphocytes correlates with disability score in multiple sclerosis patients. *Mult. Scler.* **6**, 19–23 (2000).
39. Brand-Schieber, E. *et al.* Connexin43, the major gap junction protein of astrocytes, is down-regulated in inflamed white matter in an animal model of multiple sclerosis. *J. Neurosci. Res.* **80**, 798–808 (2005).
40. Markoullis, K. *et al.* Disruption of oligodendrocyte gap junctions in experimental autoimmune encephalomyelitis. *Glia.* **60**, 1053–1066 (2012).
41. Lutz, S. E. *et al.* Deletion of astrocyte connexins 43 and 30 leads to a dysmyelinating phenotype and hippocampal CA1 vacuolation. *J. Neurosci.* **29**, 7743–7752 (2009).
42. Ezan, P. *et al.* Deletion of astroglial connexins weakens the blood-brain barrier. *J. Cereb. Blood Flow Metab.* **32**, 1457–1467 (2012).
43. Boulay, A. C. *et al.* Immune quiescence of the brain is set by astroglial connexin 43. *J. Neurosci.* **35**, 4427–4439 (2015).
44. Zhang, G. X., Baker, C. M., Kolson, D. L. & Rostami, A. M. Chemokines and chemokine receptors in the pathogenesis of multiple sclerosis. *Mult. Scler.* **6**, 3–13 (2000).
45. Yamasaki, R. *et al.* Differential roles of microglia and monocytes in the inflamed central nervous system. *J. Exp. Med.* **211**, 1533–1549 (2014).
46. Matuszewicz, D. *et al.* Interleukin-17 mRNA expression in blood and CSF mononuclear cells is augmented in multiple sclerosis. *Mult. Scler.* **5**, 101–104 (1999).
47. Brucklacher-Waldert, V., Stuermer, K., Kolster, M., Wolthausen, J. & Tolosa, E. Phenotypical and functional characterization of T helper 17 cells in multiple sclerosis. *Brain.* **132**, 3329–3341 (2009).
48. Wen, S. R. *et al.* Increased levels of IL-23 and osteopontin in serum and cerebrospinal fluid of multiple sclerosis patients. *J. Neuroimmunol.* **244**, 94–96 (2012).
49. Tzartos, J. S. Interleukin-17 production in central nervous system-infiltrating T cells and glial cells is associated with active disease in multiple sclerosis. *Am. J. Pathol.* **172**, 146–155 (2008).
50. Cua, D. J. *et al.* Interleukin-23 rather than interleukin-12 is the critical cytokine for autoimmune inflammation of the brain. *Nature.* **421**, 744–748 (2003).
51. Langrish, C. L. *et al.* IL-23 drives a pathogenic T cell population that induces autoimmune inflammation. *J. Exp. Med.* **201**, 233–240 (2005).
52. Kurschus, F. C. *et al.* Genetic proof for the transient nature of the Th17 phenotype. *Eur. J. Immunol.* **40**, 3336–3346 (2010).
53. Hirota, K. *et al.* Fate mapping of IL-17-producing T cells in inflammatory responses. *Nat. Immunol.* **12**, 255–263 (2011).
54. Murphy, A. C., Lalor, S. J., Lynch, M. A. & Mills, K. H. Infiltration of Th1 and Th17 cells and activation of microglia in the CNS during the course of experimental autoimmune encephalomyelitis. *Brain Behav. Immun.* **24**, 641–651 (2010).
55. Kebir, H. *et al.* Preferential recruitment of interferon- $\gamma$ -expressing T<sub>H</sub>17 cells in multiple sclerosis. *Ann. Neurol.* **66**, 390–402 (2009).
56. Lee, Y. K. *et al.* Late developmental plasticity in the T helper 17 lineage. *Immunity.* **30**, 92–107 (2009).
57. Annunziato, F. & Romagnani, S. The transient nature of the Th17 phenotype. *Eur. J. Immunol.* **40**, 3312–3316 (2010).
58. Suzumura, A., Bhat, S., Eccleston, P. A., Lisak, R. P. & Silberberg, D. H. The isolation and long-term culture of oligodendrocytes from newborn mouse brain. *Brain. Res.* **324**, 379–383 (1984).
59. el-Fouly, M. H., Trosko, J. E. & Chang, C. C. Scrape-loading and dye transfer. A rapid and simple technique to study gap junctional intercellular communication. *Exp. Cell Res.* **168**, 422–430 (1987).

## Acknowledgements

This study was supported in part by a Health and Labour Sciences Research Grant on Intractable Diseases (H26-Nanchitou (Nan)-Ippan-074) from the Ministry of Health, Labour, and Welfare, Japan, the Practical Research Project for Rare/Intractable Diseases from Japan Agency for Medical Research and Development (AMED), a “Glial assembly” Grant-in-Aid for Scientific Research on Innovative Areas (MEXT KAKENHI Grant Numbers 25117001 and 25117012) from the Ministry of Education, Culture, Sports, Science and Technology of Japan, a Grant-in-Aid for Scientific Research (A) (JSPS KAKENHI Grant Number 16H02657), a Grant-in-Aid for Scientific Research (C) (JSPS KAKENHI Grant Numbers 16K09694 and 26461295), a Grant-in-Aid for Exploratory Research (JSPS KAKENHI Grant Number 15K15341), and a Grant-in-Aid for Young Scientists (B) (JSPS KAKENHI Grant Number 15K19489) from the Japan Society for the Promotion of Science. We appreciate the assistance from The Research Support Center, Research Center for Human Disease Modeling, Kyushu University Graduate School of Medical Sciences.

## Author Contributions

M.W. and J. Kira conceived the experiments. All authors contributed to the experimental design. M.W. performed the experiments and analysed the results. J. Kawanokuchi, H.T., and A.S. provided technical advice for the experiments. M.W., K.M., R.Y., T.M., and J. Kira were involved in the interpretation of results. M.W., K.M., and J. Kira drafted the manuscript. All authors reviewed the manuscript.

## Additional Information

**Supplementary information** accompanies this paper at <http://www.nature.com/srep>

**Competing financial interests:** T.M. has received honoraria from Bayer Schering Pharma, Biogen Idec, Takeda Pharmaceutical Company, and Mitsubishi Tanabe Pharma; J. Kira is a consultant for Biogen Idec Japan, Novartis Pharma A.G., and Medical Review. He has received speaking fees and/or honoraria from Bayer Healthcare, Mitsubishi Tanabe Pharma, Nobelpharma, Otsuka Pharmaceutical, Novartis Pharma K.K., Takeda Pharmaceutical Company, Nippon Rinsho, and Medical Review. He has received grants from Pfizer, Eisai, Japan Blood Products Organization, Mitsubishi Tanabe Pharma, and Bayer Healthcare; the other authors declare no conflicts of interest.

**How to cite this article:** Watanabe, M. *et al.* Th1 cells downregulate connexin 43 gap junctions in astrocytes via microglial activation. *Sci. Rep.* **6**, 38387; doi: 10.1038/srep38387 (2016).

**Publisher's note:** Springer Nature remains neutral with regard to jurisdictional claims in published maps and institutional affiliations.



This work is licensed under a Creative Commons Attribution 4.0 International License. The images or other third party material in this article are included in the article's Creative Commons license, unless indicated otherwise in the credit line; if the material is not included under the Creative Commons license, users will need to obtain permission from the license holder to reproduce the material. To view a copy of this license, visit <http://creativecommons.org/licenses/by/4.0/>

© The Author(s) 2016